Journal of Inclusion Phenomena and Molecular Recognition in Chemistry **11**: 71–88, 1991.

Molecular Dynamics Simulations on the Protonated 222. H^+ and 222. $2H^+$ Cryptands in Water: *Endo* versus *exo* Conformations

P. AUFFINGER and G. WIPFF*
Institut de Chimie, 1 rue Blaise Pascal 67000 Strasbourg, France.

(Received: 17 January 1991; in final form 17 April 1991)

Abstract. MD simulations on the 222 cryptand, monoprotonated 222. H^+ and diprotonated 222. $2H^+$ in the *endo-endo* and *exo-exo* conformations have been performed *in vacuo* and in a bath of water molecules. It is found that intrinsically *endo* protonation is favoured over *exo* protonation due to internal N—H^+···O hydrogen bonding which makes the cage more rigid. On the other hand, *endo* protonated forms display 'hydrophobic' hydration compared to *exo* forms. For the monoprotonated 222. H^+ *endo* conformer, one water molecule is hydrogen bonded inside the cage thereby forming a 'water cryptate'. From the hydration pattern found previously for the neutral 222 cryptand and for its cation complexes, we suggest mechanisms (not involving *exo* to *endo* conversions) for the protonation of 222 and for acid catalysed decomplexation of cryptates in the *endo-endo* form.

Key words. Cryptands, recognition, protonation, molecular dynamics, solvation, molecular modelling.

1. Introduction

Since the synthesis of the 222 cryptand by Dietrich, Sauvage and Lehn [1, 2], the determination of its conformation appeared to be essential for understanding the detailed mechanisms of complexation and decomplexation of various cations in solution. By analogy with the bicyclic polyamines studied by Simmons and Park [3] much attention has been paid to the orientation of the nitrogen lone pairs which can be schematically *endo-endo*, *endo-exo*, or *exo-exo* (Figure 1). There have been few discussions on the orientation of the oxygen binding sites. In the cryptates, they converge to the guest cation to achieve optimal steric and electrostatic complementarity, as has been confirmed by X-ray crystallographic studies [5]. In the solid state the free cryptand adopts an *endo-endo* conformation of nitrogen bridgeheads, quite elongated and without a preformed cavity [6], but its precise conformation in solution is not known from experiment [1]. Molecular modelling techniques can provide significant insights into the conformational preferences of macrocyclic receptors *in vacuo* and molecular mechanics (MM) calculations were used to compare the relative stabilities of experimental and modelbuilt forms of the 222 cryptand and cryptates [7]. Geue *et al.* reported a similar study for the 111 and 222 cryptands [8]. We also performed molecular dynamics (MD) simulations on crown ethers, cryptands and cryptates *in vacuo* at 300 K to obtain dynamic views on the questions of preorganization, dynamics and complementarity [9]. More recently, MD simulations on 222 cryptand and cryptates in water [10] led us to conclude that

* Author for correspondence

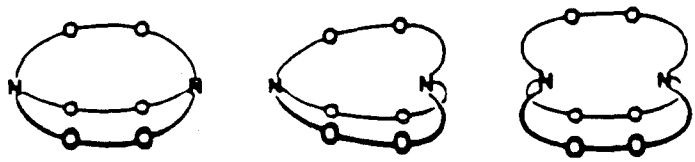

Fig. 1. Schematic representations of *exo-exo*, *exo-endo*, and *endo-endo* forms of 222.

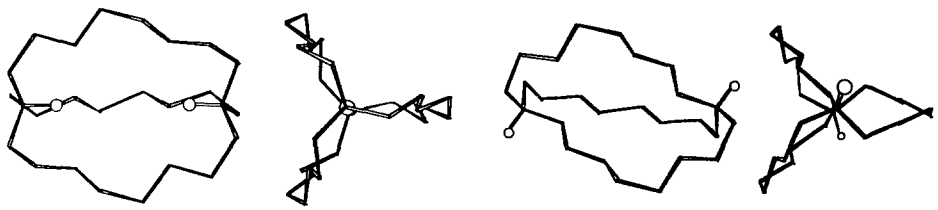

Fig. 2. Orthogonal views of the diprotonated *K*. $2H^+$ (*endo-endo*) and *OO*. $2H^+$ (*exo-exo*) conformers of the 222 cryptand.

among different conformers of neutral 222 extracted from solid state structures, the *endo-endo* conformer of the K^+ cryptate [11] was significantly better hydrated than other *endo-endo* or *exo-exo* conformers and should therefore have a high population in aqueous medium [10]. There have been, to our knowledge, no such theoretical studies on the protonated forms of 222.

Here, we address, using MD simulations, the question of hydration and dynamics of mono- and di-protonated 222, and compare typical *endo-endo* and *exo-exo* forms in order to gain insights into their relative stabilities. This question is of relevance to the detailed mechanisms for protonation, proton transfer [12–16] and of decomplexation of cryptates in acidic conditions [13, 17–20]. For this purpose, two representative conformers extracted from solid state structures are considered. The *endo-endo* form, denoted *K* in the following discussion corresponds to the K^+ cryptate which is the most stable alkali cation complex formed by 222. In the cavity left by K^+, a proton or H_3O^+ (by analogy with NH_4^+[21]) can fit without steric constraint. For the *exo-exo OO* form (this notation stands for 'out-out', synonymous with 'exo–exo' [4]), we used the structure of the bis-BH_3 adduct of 222 [6]. The corresponding acids will be denoted as *K*. H^+ or *OO*. H^+ for the monoprotonated states, and *K*. $2H^+$ or *OO*. $2H^+$ for the diprotonated states (Figure 2).

2. Methods of Calculations

Molecular dynamics calculations were performed with the program AMBER 3.0 [22], using the following representation of the potential energy [23]:

$$E_T = \sum_{\text{bonds}} K_r(r - r_{\text{eq}})^2 + \sum_{\text{angles}} K_\theta(\theta - \theta_{\text{eq}})^2$$

$$+ \sum_{\text{dihedrals}} (1 + \cos(n\phi - \gamma)) + \sum_{i<j} \{B_{ij}/R_{ij}^{12} - A_{ij}/R_{ij}^{6} + q_i q_j/\varepsilon R_{ij}\}$$

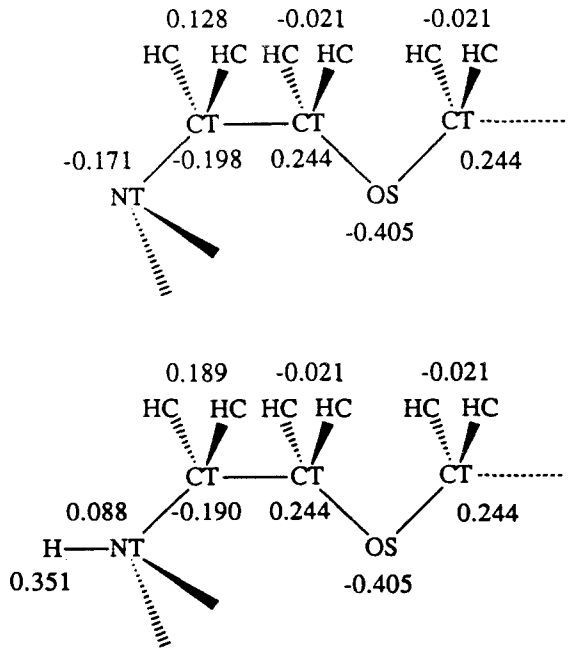

Fig. 3. Charges and atom types for the $-N-CH_2-CH_2-O-CH_2-$ and $^+H-N-CH_2-CH_2-O-CH_2-$ moieties of 222.

The bonds and bond angles are treated as harmonic springs, and a torsional term is associated to the dihedral angles. The interactions between atoms separated by at least three bonds are described by a pairwise additive 1–6–12 potential. The parameters are taken from the AMBER all atom force field [23] as used in the calculation on neutral 222 [24]. The atomic charges used here have been fitted on electrostatic potentials calculated *ab initio* at the 6-31G* level on representative fragments as used for the SC24 receptor [25]. They are reported in Figure 3.

For simulations in solution, the TIP3P potentials of water [26] were used. Each conformer has been placed at the center of a cubic box of water, 30 Å in length. Removal of the solvent molecules at contact left respectively 820, 823, 815, 820 water molecules for *K*. $2H^+$, *OO*. $2H^+$, *K*. H^+ and *OO*. H^+. After 100 steps of molecular mechanics optimization, the systems were equilibrated for 6 ps of MD at 300 K and 1 atmosphere starting with random velocities. This was followed by 45 ps of MD. Periodic boundary conditions were applied with a residue based cut-off of 8.0 Å for non-bonded interactions. The Verlet algorithm was used with a time step of 2 fs. The C—H bonds of 222 and the O—H and H···H distances of H_2O were constrained to constant values by SHAKE [27]. Coordinates were saved every 0.02 ps and subjected to further structural and energy analysis. Each simulation took about 20 hours on an IBM-3090 VF. A similar procedure was used for consistency, for the simulations *in vacuo* performed for comparison.

The MDNM graphics software allowed us to dynamically visualize the hydration pattern [28]. Plots of radial distribution functions, and calculation of solute/solvent

interaction energies were performed using adapted analysis modules of GROMOS [29] which were interfaced to AMBER output.

3. Results

3.1. STRUCTURE AND DYNAMICS OF 222. nH^+ IN VACUO

Protonation affects both the relative stabilities and dynamic properties of *endo* 222 compared to the *exo* conformer (Table I). The first protonation significantly stabilizes the *endo*, relative to the *exo* form. Whereas *K* neutral is calculated with this force field to be about 8 kcal/mol less stable than *OO*, mono and diprotonations make the *endo* form more stable than the *exo* form, by 9 and 21 kcal/mol, respectively. We anticipated that proton–proton repulsion would make the second *endo* protonation relatively more difficult than *exo*, but this is clearly not the case. A primary reason is that the positive charge is delocalized over the bridgehead atoms of 222 rather than being localized on the protons (Figure 2). Secondly, the protonated *K* form is stabilized by internal N—H^+···O hydrogen bonding (shown schematically in Figure 4). The corresponding distances are about 2.4 Å after MM optimization and about 2.8 Å on the average after 45 ps of MD (Table II). In the diprotonated *endo* form, the MM optimized and MD average proton-proton distances are respectively 4.4 Å and 5.1 ∓ 0.7 Å.

This internal hydrogen bonding makes the *endo* form more rigid, as seen from the MD results. Upon mono- and diprotonation, the atomic fluctuations drop from 0.72 Å (in the neutral form) to 0.68 and 0.48 Å, respectively, and the number of dihedral transitions decreases from 64 to 41 and 3, respectively (Table III). For the *exo* form, the stiffening which occurs upon protonation is significantly weaker (Table III). One also observes that the *gauche* NC—CO and OC—CO dihedral angles are smaller in *K*. $2H^+$ than in neutral *K*, a result consistent with the N—H^+···O attractions (Table IV).

Table I. Energy component analysis after the MD simulations in water.

Solute	*K*. $2H^+$	*OO*. $2H^+$	*K*. H^+	*OO*. H^+	*K*	*OO*
$\langle E_{sw} \rangle^{ab}$	−239 (12)	−279 (12)	−127 (9)	−134 (8)	−79 (5)	−48 (5)
$\langle E_{solute} \rangle$	90 (4)	110 (4)	41 (4)	45 (4)	39 (4)	29 (4)
$\Delta E_{opt.}{}^{c}$	58	79	4	13	9	1
$\langle E_{ww} \rangle$	−7813 (79)	−7818 (83)	−7912 (85)	−7872 (80)	−7939 (81)	−7886 (82)
$\langle E_{ww} \rangle^{d}$	−7803	−7780	−7950	−7862	−7939	−7944
E_{total}	−7952	−7949	−8037	−7951	−7979	−7963
Contribution of the 6 Oxygens, 2 Nitrogens, 18 CH_2 and (N)—H^+ protons to E_{sw}						
O	234 (16)	251 (16)	90 (19)	100 (16)	−89 (16)	−48 (20)
N	−21 (1)	−24 (1)	−6 (1)	−6 (1)	−9 (2)	−5 (2)
CH_2	−378 (12)	−400 (12)	−181 (12)	−185 (12)	19 (12)	5 (12)
H^+	−24 (4)	−106 (6)	−30 (3)	−43 (3)	/	/

[a]Energies (kcal/mol) are calculated with a cut-off of 8 Å for E_{ss} and E_{sw}
[b]Fluctuations are given in parenthesis.
[c]Relative energies for the cryptands optimized *in vacuo*.
[d]Energy corrected for 819 water molecules.

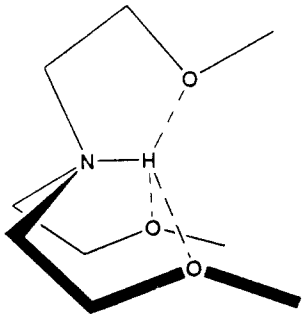

Fig. 4. Scheme for internal hydrogen bonding in the *endo* protonated 222 cryptand.

Table II. Average distances (Å) from the MD simulations *in vacuo* and in water, and optimized *in vacuo* for the *endo-endo* forms of the 222 cryptand.[a]

	$d_{N\cdots N}$			$d_{NH^+\cdots+HN}$			$d_{NH^+\cdots Ob}$		
	⟨Vac⟩	⟨Soln.⟩	Opt.	⟨Vac.⟩	⟨Soln.⟩	Opt.	⟨Vac.⟩	⟨Soln.⟩	Opt.
K. 2H	7.4 (1.0)	7.3 (1.0)	6.5	5.1 (0.7)	5.0 (0.7)	4.4	2.8 (0.4)	2.8 (0.4)	2.4
K. H^+	6.3 (0.9)	7.0 (0.9)	5.3	/	/	/	2.9 (0.4)	3.0 (0.4)	2.5
K	6.1 (0.3)	5.9 (0.2)	6.5	/	/	/	/	/	/

[a]Fluctuations are in parenthesis.
[b]Distance between the N–H^+ proton and the three adjacent oxygens.

Table III. Average of the root mean square atomic fluctuations (Å) and number of dihedral transitions (in parenthesis) from the MD simulations *in vacuo* and in water for *endo-endo* (*K*) and *exo-exo* (*OO*) conformers.

Forms	*K*. $2H^+$	*OO*. $2H^+$	*K*. H^+	*OO*. H^+	*K*	*OO*
Vac.	0.48 (3)	0.52 (19)	0.68 (41)	0.71 (58)	0.72 (64)	0.65 (34)
Aq.	0.52 (2)	0.23 (23)	0.39 (6)	0.29 (1)	0.31 (0)	0.46 (5)

Table IV. Dihedral angles of *endo-endo* neutral and diprotonated 222: average MD values in water and values optimized *in vacuo*.

	K. $2H^+$		*K* neutral	
	⟨in water⟩[a,b]	optimized	⟨in water⟩[a]	optimized
NC—CO	−57.2 (92)	−59.5	−63.3 (9.3)	−71.3
OC—CO	66.0 (12.2)	72.6	54.0 (10.1)	82.8
CC—OC	178.1 (17.2)	179.0	−179.8 (10.5)	175.8
CC—NC[c]	159.8 (11.6)	157.8	163.1 (7.9)	154.6
CC–NC[c]	−78.1 (10.6)	−81.2	−69.0 (8.6)	−82.9

[a]Fluctuations are in parenthesis.
[b]Averages during the first 39 ps where no conformational transition occur.
[c]There are six *gauche* and six *trans* CC—NC dihedral angles.

3.2. STRUCTURE AND DYNAMICS OF 222. nH^+ IN WATER

In water the solutes undergo limited conformational changes compared to the gas phase where many changes occur. It is therefore difficult to compare the average structures in the gas phase and in water. In water, the average conformation of the *endo-endo* diprotonated form remains similar to that optimized *in vacuo* for the first 39 ps of the simulation (Table IV). Then, some dihedral transitions occur. For the other protonated species, we find also that the average structures in water do not differ much from the optimized ones. Because they lack D_3 symmetry, the list of dihedral angles would be too long, and has not been reported in Table IV.

There are interesting changes in the dynamics behaviour, from the gas phase to the aqueous solution, and for the *endo*, compared to the *exo* form (Table III). For the *exo-exo* conformer, the fluctuations are reduced in water, compared to the gas phase and are smaller in the protonated states (respectively 0.29 and 0.23 Å) than in the neutral form (0.46 Å). For the *endo-endo* neutral or monoprotonated form, the motions are also reduced upon hydration but the diprotonated form is more mobile in water than in the gas phase. We have shown previously [10] that in the neutral state the *K* form is stiffened by a particular hydration pattern with three water molecules held by hydrogen bonds between the bridges of 222 (shown schematically in Figure 5) giving rise to 'solvent induced strain'. On the other hand, the fact that the diprotonated *endo-endo* form is somewhat more mobile in water than in the gas phase is consistent with a competition between intramolecular $N—H^+\cdots O$ and intermolecular $N—H^+\cdots OH_2$ interactions in water.

3.3. SOLUTE–WATER INTERACTION ENERGIES

The solute–water interaction energies E_{SW} have been calculated for each set of coordinates saved after the MD simulation, including all water molecules within 8 Å of the solute (Table I). The results are consistent with a conformation and protonic state dependent specific hydration.

As expected, *exo* protons are more accessible to solvation than *endo* protons, and *OO*. H^+ or *OO*. $2H^+$ is better hydrated than the corresponding *K*. H^+ or *K*. $2H^+$. The *exo* versus *endo* stabilization by water amounts to -31 kcal/mol for neutral 222, 7 kcal/mol for 222. H^+ and 40 kcal/mol for 222. $2H^+$. These ΔE_{SW} energies are thus, within statistical fluctuations, in a roughly linear relationship with the number of protons *n*. It is noticeable, however, that the ΔE_{SW} for *endo-endo* compared to *exo-exo* is more than twice as large for $n = 2$ (40 kcal/mol) than for $n = 1$ (7 kcal/mol). This results from two effects: (i) better hydration of *OO*. $2H^+$ compared to *K*. $2H^+$ (ii) specific stabilization by water of *K*. H^+, not present in *OO*. H^+. It will be shown (see next section) that the (N)—H^+ *endo* proton of *K*. H^+ is strongly hydrogen bonded to one water molecule held inside the cage, whereas for *K*. $2H^+$, the *endo-endo* topology prevents significant hydrogen bonding to water. By contrast, *exo* (N)–H^+ protons are in direct contact with the solvent.

Dissection of E_{SW} into the contributions of the 6 oxygens, 2 nitrogens, 18 CH_2 and (N)–H^+ groups of the cryptand supports this simple explanation based on

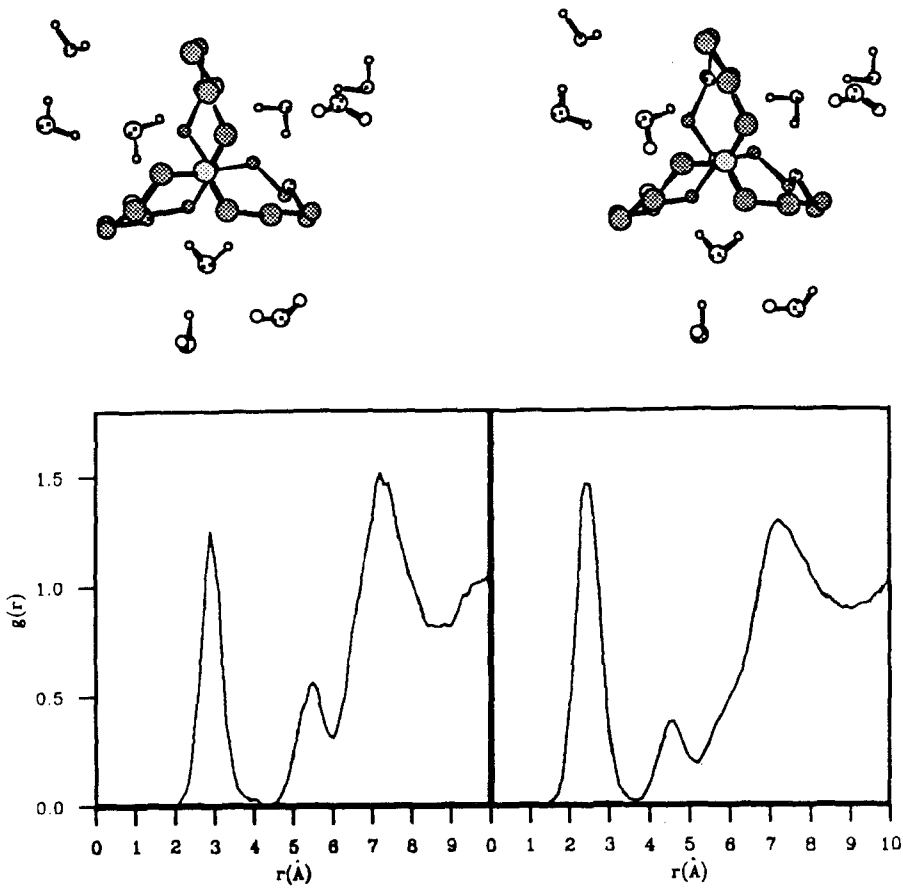

Fig. 5. Stereoview of the hydrated *K* form, and radial distribution functions of water (O_W left and H_W right) around its center of mass (CM) [10].

(N)–H^+ accessibility (Table I). The (N)–H^+ contribution to E_{SW} is more negative in the *exo-exo* than in the *endo-endo* form (by 13 kcal/mol for 222. H^+ and by 32 kcal/mol for 222. $2H^+$). There are, however, significant changes in the other components from *endo-endo* to *exo-exo* as well and, for each conformation, as a function of the protonation state (Table I). For instance, the 18 CH_2 contribution, slightly repulsive in the neutral forms (19 and 5 kcal/mol, respectively) becomes attractive upon monoprotonation (-181 and -185 kcal/mol respectively) and upon diprotonation (-378 and -400 kcal/mol) of 222. There is also a dramatic evolution of the contribution of the 6 oxygen atoms to E_{SW}, which is attractive for neutral 222 (-89 and -48 kcal/mol), but becomes repulsive for 222. H^+ (90 and 100 kcal/mol) and for 222. $2H^+$ (234 and 251 kcal/mol). These numbers indicate that the hydration of 222 is mostly driven by the N···H—OH and O···H—OH hydrogen bonds for neutral 222 and by the electrostatic interactions between water and the $+1$ or $+2$ charge of the solute in the protonated forms. The total water–water interaction energy E_{SW} becomes less and less negative for the

exo-exo forms as the charge of the solute increases (Table I), a trend found for spherical cations (Na^+, Ca^{2+}, Eu^{3+}) uncomplexed in water [10]. The decrease of E_{sw} brought about upon successive protonations of the *endo-endo* and *exo-exo* forms is respectively 48 and 86 kcal/mol (from mono- to diprotonated). As a result, the *endo-endo* form which was better hydrated that the *exo-exo* form in the neutral state becomes less well hydrated after protonation.

The water–water interaction energies E_{ww} (Table I) are large numbers with significant fluctuations (about 80 kcal/mol). They can therefore be considered, within this statistical error, to be comparable from one conformer to the other with the same charge. A trend is found, however, for water–water destabilization upon successive protonations of one given form, in the order of 80 kcal/mol from *OO* to *OO*. $2H^+$ (in a box of 819 water molecules). Increasing the charge of the solute induces some reorientation of the water dipoles relative to the solute and therefore some loss of water–water hydrogen bonds.

3.4. HYDRATION PATTERN AS A FUNCTION OF THE CONFORMATION AND OF THE PROTONIC STATE

In order to obtain more precise pictures of the hydration pattern, we performed a detailed hydrogen bond analysis, calculated the radial distribution functions, and displayed solute–water 'supermolecules' with the graphics system. The results reveal how hydration depends markedly on the protonic state and on the conformation of the solute.

Hydrogen Bond Analysis

We first investigated the occurrence of solute···HOH 'linear' hydrogen bonds in all sets of coordinates. For water as hydrogen donor, we scored all water molecules having their proton at less than 2.5 A from any oxygen or nitrogen atom of the solute and such that the corresponding O···H—O or N···H—O angles are larger than 135°. For water as proton acceptor, we scored all N—H^+···OH_2 hydrogen bonds defined similarly. Table V summarizes the percentage of such hydrogen bonds (100% would correspond to one hydrogen bond found in all sets of coordinates) and the number of water molecules involved.

The first result is the complete loss of N···HOH and O···HOH hydrogen bonds in going from neutral 222 to 222. $2H^+$ *endo* or *exo*. For the monoprotonated form 222. H^+ there are still significant hydrogen bonds, although less than in the neutral form (Table V). The second important feature is the absence of N—H^+···water hydrogen bonds for the diprotonated *endo-endo* form, in contrast to the *exo-exo* conformer which displays 69% of such bonds. The latter should be rather weak, since significant water exchange (11 water molecules during the 45 ps) occurs. For the monoprotonated cryptand 222. H^+ there appears to be again another specific conformation dependent hydration pattern for (N)—H^+. In contrast to the *exo-exo* conformer where hydrogen bonds (73.6%) involving 6 water molecules suggests relatively weak interactions there is for *K*. H^+ one permanent (99.6%) single hydrogen bonded water molecule. The display of the structures shows that it is held cooperatively (via N—H^+···HO—H···N interactions involving the unprotonated

Table V. Hydrogen bond analysis for solute/water interactions: percentage of hydrogen bonds in the saved coordinates.[a,b]

Forms	*K*. $2H^+$	*OO*. $2H^+$	*K*. H^+	*OO*. H^+	*K*	*OO*
O···HOH	0	0	52.6	33.4	93.4	61.8
N···HOH	0	0	14.9[c]	15.5	0	15.8
$NH^+\cdots OH_2$	0	68.7	99.6[c]	73.6	/	/
Total number of water molecules involved in solute/water hydrogen bonding[b]						
O	0	0	10	11	3	10
N	0	0	1[c]	3	0	3
$N–H^+$	0	11	1[c]	6	/	/

[a]100% would correspond to one hydrogen bond found in all the sets of coordinates.
[b]Hydrogen bonding was defined by the following geometrical criteria: the X···H—O distance is less than 2.5 Å, and the X···H—O angle is larger than 135°. Those occurring for less than 2% have been discarded.
[c]Hydrogen bonds involving the water molecule inside the cavity of 222. H^+.

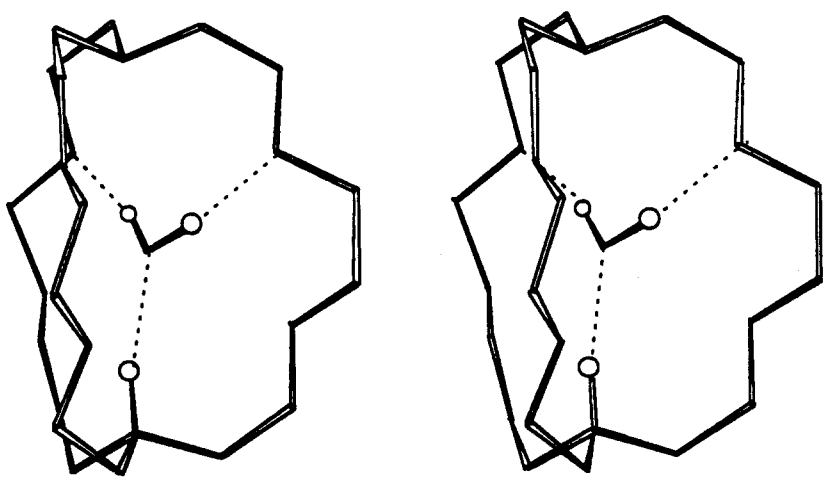

Fig. 6. The 'water cryptate' formed by 222. H^+ *endo-endo* in water.

nitrogen and $N—H^+\cdots HO–H\cdots O$ interactions involving ether oxygens) *inside* the cavity of 222. H^+ *endo-endo*, as shown in Figure 6.

Radial Distribution Functions

The radial distribution functions (rdfs) for the O_W and H_W atoms of water around the center of mass (CM) of the solutes and around the proton $(N)—H^+$ are displayed in Figure 7 for 222. H^+ and Figure 8 for 222. $2H^+$. They have to be compared with similar curves calculated for the corresponding unprotonated conformers (Figure 5) [10].

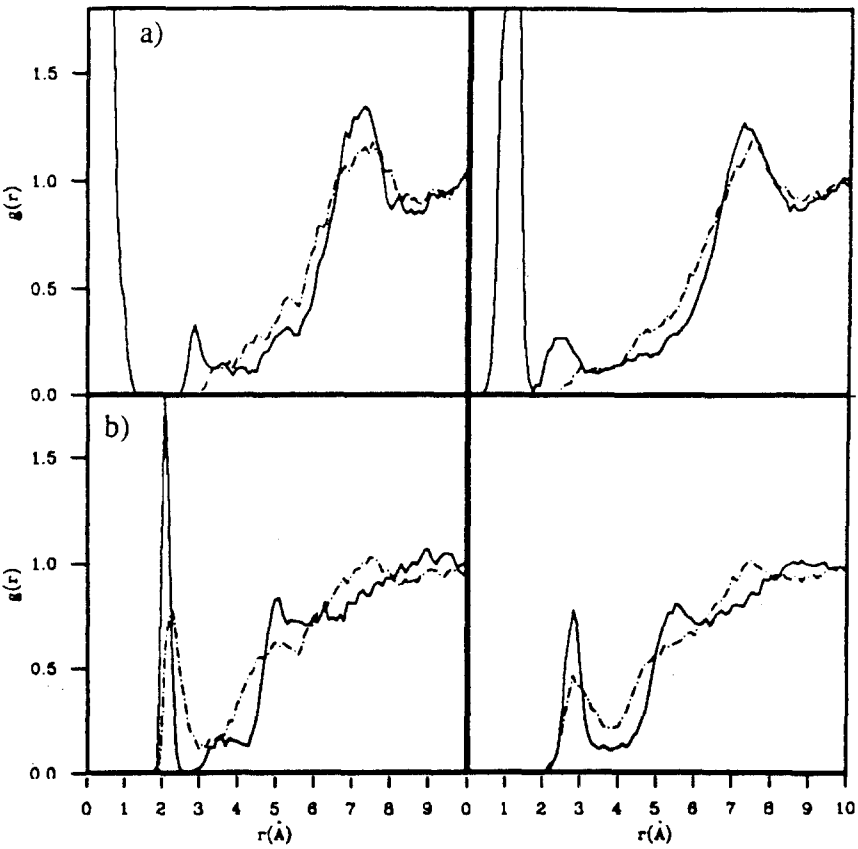

Fig. 7. The monoprotonated 222. H^+ cryptand: radial distribution functions of water (O_W left and H_W right) around: (a) its center of mass (CM), (b) the acidic hydrogen (conformations 222. H^+ *endo-endo* ———; *exo-exo* -·-·-).

Let us first consider the monoprotonated 222. H^+ forms. The CM···O_W and CM···H_W curves differ dramatically below 4 Å where the marked peaks of the *endo* form caused entirely by the water molecule held inside the cage contrast with the absence of peaks for the *exo* form. For the (N)—H^+···O_W and (N)—H^+···H_W rdfs, there is a first peak at similar distances for the two conformers, although sharper and better defined for the *exo* form. In agreement with the hydrogen bond analysis reported above; the unique water molecule inside the *endo* cage forms strong hydrogen bonds, compared with the 6 water molecules exchanging their coordination to (H)—H^+ in the *exo* form. One also observes differences in the rdfs around the oxygen, nitrogen, and CH_2 groups of 222. H^+ [30] which cannot be interpreted solely from hydration of the (N)—H^+ moiety, but result from other contributions as well, as was found in the neutral forms [10].

In the diprotonated forms 222. $2H^+$, the hydration patterns are still different (Figure 8). The CM···water rdfs are similar for the two conformers, with no marked peak at short distances. There is thus no structured water near the center of its

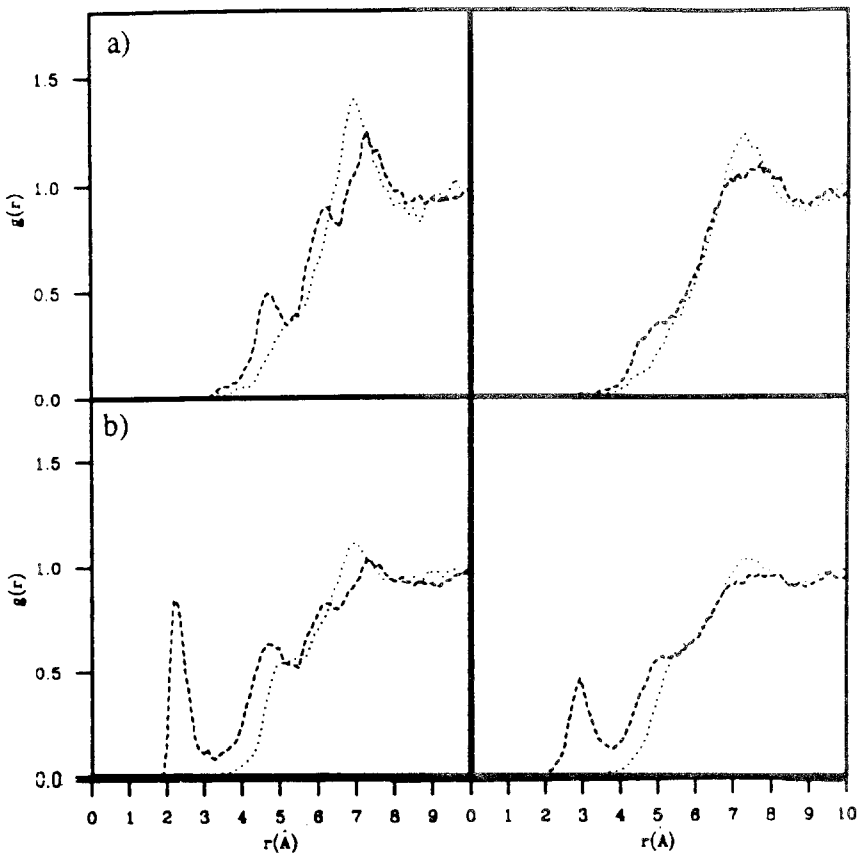

Fig. 8. The diprotonated 222. $2H^+$ cryptand: Radial distribution functions of water (O_W left and H_W right) around: (a) its center of mass, (b) the acidic hydrogens (conformations 222. $2H^+$ *endo-endo* · · ·; *exo-exo* — — —).

cavity. One might have anticipated that the two protons inside *endo* 222. $2H^+$ would attract water, as do cations encapsulated by 222 [10]. This is not consistent with our rdfs. The first important peak around 7 Å is broad and may correspond to water near the CH_2 groups, as was found in the neutral *exo-exo* form. It corresponds to the cut-off region, and must be interpreted with caution. A similar peak was also obtained in the MD simulation of the highly charged SC24. $4H^+$ in water [31]. Despite its 2^+ charge the *endo-endo K*. $2H^+$ cryptands thus behaves like a big hydrophobic rather than like a polar solute. This contrasts with the marked peak which was observed around 3 Å for the neutral *endo-endo K* form [10]. Whereas the oxygens and CH_2 rdfs appear very similar for the two conformers [30], there is a dramatic difference for the (N)—H^+ rdfs. They display no evidence of direct water coordination to the bridgeheads of the *endo-endo* form, in contrast with the *exo-exo* form (see the clear peak at 2.2 Å in the (N)—$H^+ \cdots O_W$ rdf, and at 2.8 A in the (N)—$H^+ \cdots H_W$ rdf). Integration of these peaks gives an average of 1.2 water molecules per (N)—H^+ site which is hydrogen bonded (as defined by the

geometrical criteria above) in only 68% of the saved sets of coordinates. These numbers confirm that hydration of *exo* (N)—H^+, although hydrophilic, is achieved via relatively weak and labile hydrogen bonds and by electrostatic interactions not fulfilling the geometrical requirements for optimal bonding.

The size of the *endo-endo* cage, as measured by the average $\langle N \cdots N \rangle$ distance may also be perturbed by hydration effects (Table II). Interestingly, in the monoprotonated form, $\langle N \cdots N \rangle$ increases significantly (by 0.7 Å) in water, as a result of the formation of a 222. H^+/H_2O cryptate. This contrasts with the neutral and diprotonated forms, where from the gas phase to the aqueous solution, $\langle N \cdots N \rangle$ decrease only slightly (by 0.1 to 0.2 Å).

4. Discussion

4.1. CHOICE OF STRUCTURES

We have reported molecular dynamics studies on the hydration of the 222 macrobicyclic receptor in its protonated states for typical *endo-endo* and *exo-exo* conformations. No *endo-exo* mixed form was considered, although several of them were shown to be in the gas phase a few kcal/mol only above the most stable *endo-endo* form [24]. They were not considered here, because we wanted to start from X-ray experimental structures, rather than from model-built ones. There has been, to our knowledge, no *endo-exo* structure reported so far for the 222 cryptand, or for its cryptates. For the *endo-endo* conformer, alternative experimental structures, extracted from cryptates, could have been considered. We feel that *K* is a good representative of the protonated *endo-endo* forms, since its geometry is suitable for internal N—$H^+ \cdots$O hydrogen bonding, and since the N···N distance is larger than in the Ag^+, or Ca^{2+} cryptates [5] which should reduce electrostatic repulsions between the protonated bridgeheads. It also corresponds to the K^+ cryptate, i.e. to the cation for which 222 is the most selective. Experimental structures of smaller bicyclic analogues of 222 in their protonated state have been reported. The 211. $2H^+$ [32], 111. $2H^+$ and 111. H^+ cryptands [33] are in the *endo-endo* conformation, despite the larger electrostatic repulsion between the bridgeheads resulting from shorter $^+HN \cdots NH^+$ distances (3.91 Å in 111. $2H^+$, to be compared with the optimized value of 6.5 Å in *K*. $2H^+$). In those structures, the NC—CO dihedral angles are *gauche*, as in the *K* form, and allow for internal hydrogen bonding. For the *exo-exo* conformer, we also considered the *OO* form, although alternative structures are at lower energy *in vacuo* [24]. This study is thus far from being exhaustive, since for the protonated forms, the structures underwent limited conformational changes during the MD simulation in water. As simulated recently for 18-crown-6 by MD [34], much longer simulation times would be required to 'completely' sample the conformational space (but still without convergence after 1.5 ns).

MD simulations do not allow for bond making and bond breaking processes and the pyramidal conformation at the bridgeheads is retained during the simulation. Although, X-ray structures of pyridino analogues of 222 have been reported [35] with planar nitrogen as bridgeheads, we feel that these may not be good structure representatives of 222, because of the rigidity imposed by the pyridino groups and

the *trans* conformation of the NC—CO dihedrals, leading to non convergent binding sites.

Our model does not take into account counterion and ion pairing effects. It assumes that anions do not interact directly, or at short range with the protonated solute. This is a simplification, and one could expect such interactions for the *exo-exo* forms more than for the *endo-endo* forms. There are, to our knowledge, no reports on this important point for 222. In the crystalline state of the 111. $2H^+$/picrate [33] and 211. $2H^+$/perchlorate [32] related structures, the anions are not in contact with the protonated moieties.

4.2. ENERGY RESULTS

The energy results depend on this force field representation, particularly on the choice of charges. However, as far as relative energies for the same system are concerned, this choice is less critical than for calculating absolute energies [36].

The meaningful thermodynamic quantity is the relative free energy for various conformers, involving enthalpy and entropy components. This is not accessible from the simulations because of restricted conformational sampling and statistical uncertainties. One could in principle use the free energy perturbation technique for macrocyclic compounds [34, 37–43] to compare two conformers of the same nature (e.g. 222. nH^+ *endo-endo* versus *exo-exo*) or successive protonations of the same conformer (e.g. 222. H^+ versus 222. $2H^+$). This would not lead to meaningful results in the present case. Indeed *endo* to *exo* conversion leads to a complete conformational change of the solute and would require very extensive sampling for the intermediate non-physical states. On the other hand, step by step growth of a proton at nitrogen would cause a smaller structural perturbation, but the neglect of long range electrostatic interactions cannot be simply accounted for by the Born correction [44]. Such a procedure used to assess relative pK_as of the SC24 cryptand [45] or of calixarenes [46], led to values not in agreement with experiment and cannot therefore confidently be used for prediction purposes.

We unfortunately cannot be conclusive about the preferred conformation of the protonated forms of 222 in water. We have no access to the entropic component of the free energy which might be of importance for conformational stabilities as for bonding selectivities [47]. The relative enthalpies $\Delta\Delta H$ are also difficult to compute, due to statistical uncertainties in E_{sw} and in E_{ww} (Table I). In addition the water–water interaction energies E_{ww} depend on the number of water molecules considered (either within the cut-off distances, or within the whole simulation box). This is why the 'total' energy reported in Table I is only indicative and comparable for the two conformers.

Our study provides however evidence for opposite effects on the conformation in water. Intrinsically, the *endo* protonation at the bridgehead nitrogen is favoured over *exo* protonation when the conformation of the $N(C—CO)_3$ moiety allows for internal hydrogen bonding. Similar preference was calculated *in vacuo* for the tetraprotonated SC24. $4H^+$ cryptand uncomplexed: its $(endo)_4$ conformation is prefered over $(exo)_4$ conformation because of multiple internal $NH^+\cdots O$ hydrogen bonding which compensate largely the proton-proton repulsions [48]. On the other

hand, hydration is most effective for the *exo-exo* protonated form, in contrast to what we found for neutral 222 [10].

4.3. THE 222. H^+ WATER CRYPTATE

The 'water cryptate' produced by the MD simulation on *endo* 222. H^+ presents interesting structural analogies with other experimentally or computationally characterized water adducts of macrocyclic compounds. The complexed water molecule has H_W bound to the heteroatoms of 222 and O_W bound to NH as in Reinhoudt's pyridinium crown ethers [49]. Similar three point anchoring of water has been reported in crown ethers with carboxylic protons [50] or with phenolic protons [51].

For other X-ray structures of neutral molecules bound to macrocyclic receptors, see References [52] and [53]. In the Li^+ perchlorate complex of 18-crown-6, one water molecule is held inside the ring by Li^+ (which acts like (N)—H^+ here) and the ether oxygens [54]. We have also found a similar situation for the Li^+ cryptate of 222 [10] where one water molecule is held inside the cavity by Li^+ and by the cryptand. The SC24. $2H^+$ tricyclic cryptand has also been shown by NMR [55] and by MD simulations [9] to complex one water molecule by a tetrahedral array of hydrogen bonds. Electrostatic complementarity is as important as structural fit for the recognition process. Neutral 222 does not complex water in our simulations: starting from one 'water cryptate', the encapsulated water molecule moved out of the cavity to an interbridging position [10]. For the monoprotonated 222. H^+ instead, starting with water outside the cage, one of the surrounding water molecules moves inside the cage in a few ps of MD to make an inclusion complex. On the NMR time scale, it cannot be observed because of rapid exchange with the medium [56].

4.4. MECHANISMS OF PROTONATION OF THE CRYPTAND AND CRYPTATES IN WATER

Our simulations on the neutral and protonated cyptand in water allow for speculations concerning the mechanism of protonation of the *endo-endo* form of 222. We have no problem concerning the mechanism for *exo* protonation since the *exo* nitrogen lone pair is accessible to acids to a similar extent as non cyclic amines. On the other hand, extensive studies on proton-transfer reactions of 222 and other cryptands [12–15], and the thermodynamics of protonation [57, 58] have been interpreted in terms of a predominant *endo-endo* conformation. Our previous study on neutral 222 in water [10] led us to propose a high population of *endo-endo* cryptate type conformation, i.e. with a cavity suitable for K^+ complexation. Let us start with the neutral form in water and the strongly hydrogen bonded water molecules in interbridging positions shown schematically in Figure 9.

This particular structure allows for proton transfer from the acid (e.g. H_3O^+) to one of these water molecules which in turn can easily deliver one of its protons to one nitrogen lone pair. The water protons are near enough to the nitrogens (2.8 Å) [10] to transfer without significant barrier. Such a mechanism would not require significant conformational change of the solute and is supported by the study of Kjaer *et al.* [15] on the 211 cryptand. In that system, the protonation process involves direct proton transfer through the cryptand molecular framework, the

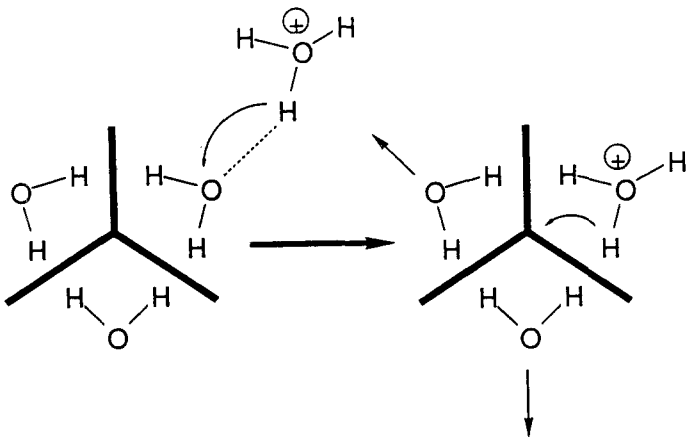

Fig. 9. Scheme proposed for protonation of the *endo-endo K* conformer of the neutral cryptand. View along the N···N axis.

proton being transferred along a water O—H to a cryptand N—H bending mode. Such a least motion pathway leads to a 'water cryptate' (Figure 6) with important reorganization of the water structure in the first hydration shell. There is particularly around $222.H^+$ no evidence of the interbridging water found around neutral 222. This is because water orientation is determined by opposing factors: its oxygen atoms are attracted by the positive charge of the $(N)—H^+$ proton, while its protons are attracted by the ether oxygens of $222.H^+$. A similar mechanism can be considered for the second protonation, involving decomplexation of the encapsulated H_2O molecule.

The decomplexation of encapsulated alkali cations can be acid-catalyzed, and interestingly more for small cations such as Na^+ or Ca^{2+}, than for bigger ones, e.g. K^+, Rb^+ or Ba^{2+}, Sr^{2+}.[20,59] It has been suggested that this would imply *exo* orientation of the nitrogen bridgeheads of the cryptate [20]. We believe that this is unlikely, because of the energy loss in cation–nitrogen interactions [7], and because nitrogen inversion in such bicyclic compounds implies conformational changes of the bridges as well, a process severely hindered by the steric strain imposed by the cation. We suggest that a bimolecular mechanism as shown schematically (Figure 10) could account for this process. A small cation such as Na^+ or Ca^{2+} is not exactly at the center of the cavity of 222, but somewhat pulled out by water [10] making the cavity accessible to direct protonation. This contrasts with K^+ or Rb^+, held at the center of the cavity for steric reasons and with a weaker hydration energy as a driving force for decomplexation. Vibration of Na^+ to one face of 222 facilitates concomitant approach of the acid to protonate the amine *endo* without significant conformational change. This scheme is fully consistent with a proposal made originally by Bemtgen *et al.* [20], according to which a proton might 'partially penetrate the cryptate cavity', particularly in the case of Ca^{2+} as compared to Sr^{2+} and Ba^{2+} [60]. Although other mechanisms involving *exo* protonation cannot be completely precluded, we feel that *exo* to *endo* conversion in the neutral or protonated states of free or complexed 222

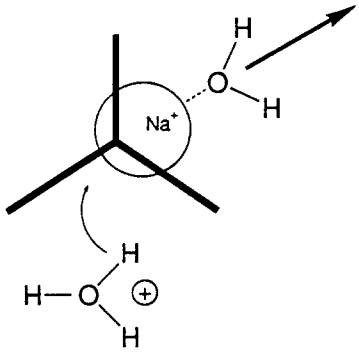

Fig. 10. Mechanism proposed for the acid catalysed decomplexation of cryptates of small cations.

would require a significantly higher activation energy than that required for nitrogen inversion only.

4.5. SOLVENT-INDUCED PREORGANIZATION

In terms of recognition and preorganization [61, 62] the 222 cryptand provides an example of a system preorganized for binding spherical ions in terms of constitution and topology, but not preorganized in terms of its conformation. The solid state structure, calculated also to correspond to 'the' absolute energy minimum in the gas phase, is not adequate for complexation, because it has no cavity. Our simulations suggest that water induces conformational changes to a conformer with a cavity complementary with K^+, i.e. to the cation which is best 'recognized' [2]. The fact that such an *endo-endo* conformer is stabilized upon protonation and allows for cation complexation, sheds light on possible 'solvent induced preorganization' of macrocyclic systems. 18-Crown-6 provides another illustration of this effect. The solid state structure of C_i symmetry is calculated to be one of the most stable in the gas phase. Monte Carlo [63] and MD [34] simulations in water provide evidence for a low population of this conformer, and for a high population of the D_{3d} form, i.e. for the form where 18-crown-6 'recognizes' K^+ among other alkali cations, forming the most stable complex. These theoretical predictions have been nicely supported by Raman spectroscopic studies on the crystalline complex between 18-crown-6 and water [64].

5. Conclusion

Molecular dynamics simulation of mono- and diprotonated *endo-endo* and *exo-exo* forms of the 222 cryptand provide information on their 'gas phase' intrinsic stabilities and on their solvation pattern in water. No conclusion can be drawn concerning which of these forms is the most stable in water, but we propose a mechanism for protonation and for acid-catalysed decomplexation of cation. This least motion mechanism involves retention of the *endo-endo* conformation, and does not require *endo* to *exo* conversion.

From the microscopic picture obtained on the hydration pattern of selected conformers, it can be stressed also that solvation depends on the size, topology and

hydrogen bonding ability of the solute. Particularly, bicyclic protonated polyamines [3] with alkyl chains may behave differently to cryptands built on $(CH_2XH_2O)_n$ units. *Endo* forms of these amines cannot be stabilized by internal hydrogen bonding, and the hydrophobic alkyl chains should be hydrated differently from ether chains. Smaller analogues of 222, like neutral or protonated 111 [33], may also display different *exo* versus *endo* preferences, not only because of reduced flexibility, but also due to different types of hydrogen bonds with water. For instance OC—CO *gauche* fragments on the three bridges of 222 allow for double hydrogen bonding with water in interbridging positions, a situation which might not be compatible with smaller analogues.

Beyond the specific cryptand studied, it is stressed that computer simulations on receptors in solution will lead to a deeper understanding of the recognition processes as an interplay of solvent dependent conformational preferences [41, 65], molecular shapes, and binding abilities.

Acknowledgements

The authors thanks Dr J.-P. Kintzinger for stimulating discussions. The CNRS-IBM Scientific Group for Molecular Modelling, and the CNRS Computer Center of Strasbourg Cronenbourg have provided the computer means for this study and are acknowledged. P. A. is also grateful to the French Ministry of Research for providing a grant. G. W. is grateful to the Région Alsace and to the Biostructure Company for funding a computer graphics workstation.

References

1. B. Dietrich, J. M. Lehn, J. P. Sauvage and J. Blanzat: *Tetrahedron* **29**, 1629 (1973).
2. B. Dietrich, J. M. Lehn and J. P. Sauvage: *Tetrahedron* **29**, 1647 (1973).
3. H. E. Simmons and C. H. Park: *J. Am. Chem. Soc.* **90**, 2428 (1968).
4. J. M. Lehn: *Struct. Bonding* **161**, 1 (1973).
5. M. Dobler in *Ionophores and their Structures.*, Editor (Eds), Wiley Interscience, New York, 1981.
6. B. Metz, D. Moras and R. Weiss: *J. Chem. Soc., Perkin Trans. 2* 423 (1976).
7. G. Wipff and P. A. Kollman: *New. J. Chem.* **9**, 457 (1985).
8. R. Geue, S. H. Jacobson and R. Pizer: *J. Am. Chem. Soc.* **108,** 1150 (1986).
9. G. Wipff and J. M. Wurtz in *Dynamic Views of Macrocyclic Receptors: Molecular Dynamics Simulations and Normal Modes Analysis*, Pullman, R. (ed.), Reidel, Dordrecht, 1988, p. 1.
10. P. Auffinger and G. Wipff: 'Hydration of the Bicylic 222 Cryptand and 222 Cryptates Studied by Molecular Dynamics Simulations', *J. Am. Chem. Soc.*, (1991).
11. B. Metz, D. Moras and R. Weiss: *J. Chem. Soc, Chem. Commun.* 444 (1971).
12. R. Pizer: *J. Am. Chem. Soc.* **100**, 4239 (1978).
13. B. G. Cox, H. Schneider and J. Stroka: *J. Am. Chem. Soc.* **100**, 4746 (1978).
14. B. G. Cox and H. Schneider: *J. Chem. Soc., Perkin Trans. 2* 1293 (1979).
15. A. M. Kjaer, P. E. Sørensen and J. Ulstrup: *J. Chem. Soc., Chem. Commun.* 965 (1979).
16. P. B. Smith, J. L. Dye, J. Cheney and J. M. Lehn: *J. Am. Chem. Soc.* **103**, 6044 (1981).
17. B. G. Cox and H. Schneider: *J. Am. Chem. Soc.* **99,** 2809 (1977).
18. B. G. Cox, D. Knop and H. Schneider: *J. Phys. Chem.* **84**, 320 (1980).
19. E. L. Yee, O. A. Gansow and M. J. Weaver: *J. Am. Chem. Soc.* **102**, 2278 (1980).
20. J. M. Bemtgen, M. E. Springer, V. M. Loyola, R. G. Wilkins and R. W. Taylor, *Inorg. Chem.* **23**, 3348 (1984).
21. B. Dietrich, J. P. Kintzinger, J. M. Lehn, B. Metz and A. Zahidi, *J. Phys. Chem.* **91**, 6600 (1987).
22. C. Singh, P. K. Weiner, J. Caldwell and P. A. Kollman; *Amber 3.0*, University of California, San Francisco (1987).

23. S. J. Weiner, P. A. Kollman, D. T. Nguyen and D. A. Case: *J. Comput. Chem.* **7,** 230 (1986).
24. P. Auffinger and G. Wipff: *J. Comput. Chem.* **11,** 19 (1990).
25. P. Grootenhuis, Personal communication (1988).
26. W. L. Jorgensen, J. Chandrasekhar and J. D. Madura: *J. Chem. Phys.* **79**, 926 (1983).
27. J. P. Ryckaert, G. Ciccotti and H. J. C. Berendsen, *J. Comput. Phys.* **23**, 327 (1977).
28. G. Wipff and J. M. Wurtz, *MDNM: a Program to Display Molecular Dynamics or Normal Modes of Vibrations on the* PS300. (1987).
29. W. F. van Gunsteren and H. J. C. Berendsen, *Groningen Molecular Simulation* (GROMOS) Library Manual Biomos, Groningen (1987).
30. P. Auffinger, Thése de Doctorat, Université Louis-Pasteur, Strasbourg (1991).
31. B. Owenson, R. D. MacElroy and A. Pohorille: *J. Am. Chem. Soc.* **110**, 6992 (1988).
32. B.. G. Cox, J. Murray-Rust, P. Murray-Rust, N. van Truong and H. Schneider, *J. Chem. Soc., Chem. Commun.* 377 (1982).
33. H. J. Brügge, D. Carboo, K. von Deuten, A. Knöchel, J. Kopf and W. Dreissig, *J. Am. Chem. Soc.* **108**, 107 (1986).
34. T. P. Straatsma and J. A. McCammon, *J. Chem. Phys.* **91**, 3631 (1989).
35. G. R. Newcome, V. Majestic, F. Fronczek and J. L. Atwood, *J. Am. Chem. Soc.* **101,** 1047 (1979).
36. S. Boudon and G. Wipff: *J. Comput. Chem.* **12**, 42 (1990).
37. T. P. Lybrand, J. A. McCammon and G. Wipff, *Proc. Natl. Acad. Sci. USA* **83**, 833 (1989).
38. J. V. van Eerden, S. Harkema and D. Feil, *J. Phys. Chem.* **92,** 5076 (1988).
39. J. van Eerden, W. J. Briels, S. Harkema and D. Feil: *Chem. Phys. Lett.* **164**, 370 (1989).
40. P. D. J. Grootenhuis and P. A. Kollman, *J. Am. Chem. Soc.* **111**, 2152 (1989).
41. W. L. Jorgensen: *Acc. Chem. Res.* **22**, 184 (1989).
42. M. H. Mazor, J. A. McCammon and T. P. Lybrand: *J. Am. Chem. Soc.* **112**, 4411 (1990).
43. L. X. Dang and P. A. Kollman: *J. Am. Chem. Soc.* **112**, 5716 (1990).
44. W. F. van Gunsteren in *On Testing Theoretical Models by Comparison of Calculated with Experimental Data.*, J. L. Rivail (Ed), Elsevier, Amsterdam, 1990, pp. 436.
45. P. D. J. Grootenhuis, P. A. Kollman, T. Malliavin and G. Wipff: Unpublished Results (1989).
46. P. D. J. Grootenhuis, P. A. Kollman, L. C. Groenen, D. N. Reinhoudt, G. J. van Hummel, F. Ugozzoli and G. D. Andreetti: *J. Am. Chem. Soc.* **112**, 4165 (1990).
47. E. Kauffmann, J. M. Lehn and J. P. Sauvage: *Helv. Chim, Acta* **59**, 1099 (1976).
48. G. Wipff and J. M. Wurtz: *New. J. Chem.* **13**, 807 (1989).
49. P. D. J. Grootenhuis, J. W. H. M. Uiterwijk, D. N. Reinhoudt, C. J. van Staveren, E. J. R. Sudhölter, M. Bos, J. van Eerden, W. T. Klooster, L. Kruise and S. Harkema: *J. Am. Chem. Soc.* **108**, 780 (1986).
50. C. J. van Staveren, V. M. L. J. Aarts, P. D. J. Grootenhuis, W. J. H. Droppers, J. van Eerden, S. Harkema and D. N. Reinhoudt: *J. Am. Chem. Soc.* **110,** 8134 (1988).
51. I. Goldberg, *Acta Crystallogr.* **B34**, 3387 (1978).
52. F. Vögtle, W. M. Müller and W. H. Watson, *Top. Curr. Chem.* **125,** 131 (1984).
53. D. N. Reinhoudt: *J. Coord. Chem.* **18,** 21 (1988).
54. P. Groth, *Acta Chem. Scand.* **A36**, 109 (1982).
55. J. M. Lehn: *Pure Appl. Chem.* **50**, 871 (1978).
56. J. P. Kintzinger: Personal communication (1990).
57. F. Arnaud-Neu, B. Spiess and M. J. Schwing-Weill, *J. Chem. Res. (S)* 10 (1982).
58. N. Morel-Desrosiers and J. P. Morel, *J. Phys. Chem.* **88,** 1023 (1984).
59. R. M. Izatt, J. S. Bradshaw, S. A. Nielsen, J. D. Lamb, J. J. Christensen and D. Sen, *Chem. Rev.* **85**, 271 (1985).
60. The authors are grateful to one of the referees who pointed out his earlier proposal.
61. D. J. Cram: *Science* **240**, 760 (1988).
62. J. M. Lehn: *Angew. Chem., Int. Ed. Engl.* **27**, 89 (1988).
63. G. Ranghino, S. Romano, J. M. Lehn and G. Wipff: *J. Am. Chem. Soc.* **107**, 7873 (1985).
64. H. Matsuura, K. Fukuhara, K. Ikeda and M. Tachikake, *J. Chem. Soc., Chem. Commun.* 1814 (1989).
65. S. Boudon and G. Wipff: 'How Important is Water in the Preoganization of Polyammonium Host Molecules', in *Advances in Biomolecular Simulations*, Troyanovski (ed.) OOOO, (1991).
G. Wipff: 'Molecular Modeling Studies on Molecular Recognition: Crown Ethers, Cryptands and Cryptates. From Static Models in vacuo to Dynamical Models in Solution' *J. Coord. Chem. B* (1991).